Effective action of the weakly doped t-J model and spin-wave excitations in the spin-glass phase of $La_{2-x}Sr_xCuO_4$

A.I. Milstein

Budker Institute of Nuclear Physics, Novosibirsk, Russia

- A. Lüscher, G. Misguich, A.I. Milstein, and O.P. Sushkov,
  Phys. Rev. **B73**, 085122, (2006)
  Local spin spirals in the Néel phase of $La_{2-x}Sr_xCuO_4$
- A. Lüscher, A.I. Milstein, and O.P. Sushkov,
  Phys. Rev. Lett. **98**, 037001, (2007)
  Structure of the spin-glass state of $La_{2-x}Sr_xCuO_4$: the spiral theory
- A. Lüscher, A.I. Milstein, and O.P. Sushkov,
  Phys. Rev. **B75**, 235120, (2007)
  Effective action of the weakly doped t-J model and spin-wave excitations in the spin-glass phase of $La_{2-x}Sr_xCuO_4$

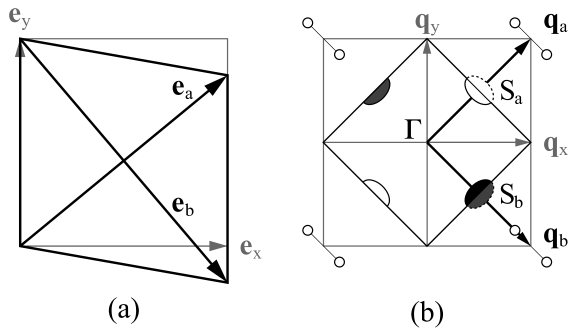

FIG. 1: *(a) Schematic drawings of a CuO_2 plane in the tetragonal and orthorhombic phase. (b) Reciprocal lattice with tetragonal and orthorhombic (for simplicity shown without distortion) unit vectors. Due to the orthorhombic distortion, holes around $S_b = \left(\frac{\pi}{2}, -\frac{\pi}{2}\right)$ have lower energy and the spirals induced by these holes are directed along the orthorhombic b-direction. This leads to the incommensurate magnetic peaks shown as small open circles.*

Ground state

The consideration is based on the effective low-energy Hamiltonian obtained within the framework of the non-linear σ-model (NLSM), where the unit vector $\vec{n}(\mathbf{r})$ is used for the staggered component of the copper spins. In insulating LSCO, holes are trapped by Sr ions and form hydrogen-like bound states

$$\psi\left(\mathbf{r}\right) = \Psi\chi\left(\mathbf{r}\right) = \Psi\sqrt{2/\pi}\kappa e^{-\kappa r},$$

where Ψ is a two-component spinor describing the pseudospin and $\kappa \approx 0.4$ is the inverse localization length.

The magnetic state of $La_{2-x}Sr_xCuO_4$ changes tremendously with Sr doping.

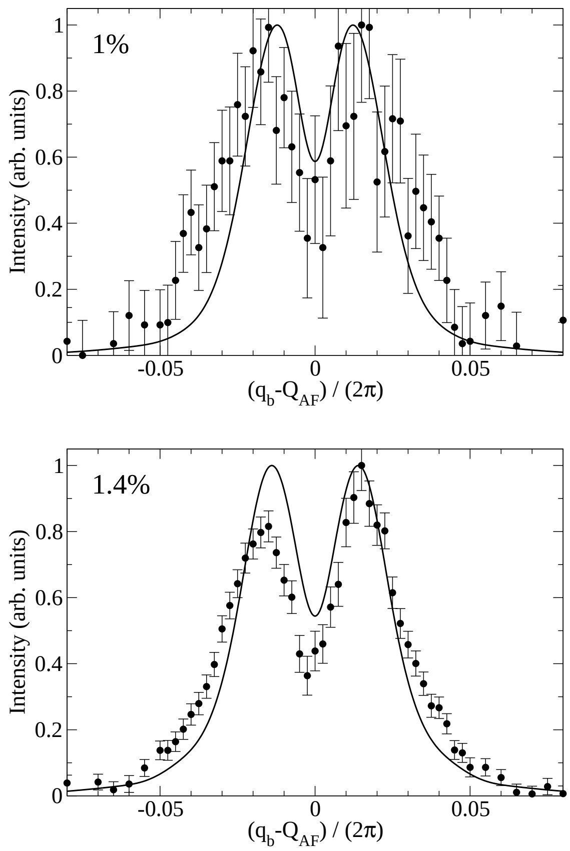

FIG. 2: *Neutron scattering probability for $x = 0.01$ and $x = 0.014$. The dots correspond to experimental observations. The curves represent our simulations convoluted with a gaussian to take into account the finite experimental resolution. The agreement between simulations (containing no fitting parameters at all) and experiments is remarkable.*

- Néel ordering and local spin spirals at $x < 0.02$.

One of the achievements: **Explanation of incommensurate neutron scattering peaks**

The experimental conditions in M.Matsuda et al (Phys. Rev. **B 65** 134515 (2002)) are such as neutrons only interact with the projections of electron spins orthogonal to the b-axis

- Spin-glass phase between $x \approx 0.02$ and $x \approx 0.055$.

We represent $\vec{n} = \left(n^a, n^b, n^c\right) = (\sin\theta, \cos\theta, 0)$. Then the energy of the effective $O(2)$ NLSM reads

$$\frac{\rho_s}{2} \int d^2 r \left\{ \left[\nabla\theta\left(\mathbf{r}\right)\right]^2 + 2\mathcal{M} \sum_i l_i \rho\left(\mathbf{r} - \mathbf{r}_i\right) \left(\mathbf{e}_b \cdot \nabla\right) \theta\left(\mathbf{r}\right) \right\}, \tag{1}$$

where $l_i = \Psi_i^\dagger \sigma^c \Psi_i$ is an Ising variable taking the values ± 1 and $\mathcal{M} = \sqrt{2} g/\rho_s \approx 8$, $\rho_s \approx 0.18J$ is the spin stiffness. This equation is valid for arbitrary θ and not restricted to small angles.

Because of the linearity of the problem,

$$\theta\left(\mathbf{r}\right) = \sum_{i=1}^{N} l_i \vartheta\left(\mathbf{r} - \mathbf{r}_i\right) \ ,$$

where

$$\vartheta\left(\mathbf{r}\right) = \frac{\mathcal{M}}{2\pi} \frac{\mathbf{e}_b \cdot \mathbf{r}}{r^2} \left\{ \left(1 + 2\kappa r\right) e^{-2\kappa r} - 1 \right\} \ . \tag{2}$$

Then we obtain the energy in terms of the Ising pseudospins l_i only

$$E_I = \frac{\rho_s \mathcal{M}^2 \kappa^2}{2\pi} \sum_{i \neq j}^{N} l_i l_j \left\{ F_1\left(\kappa r_{ij}\right) + \cos\left(2\alpha_{ij}\right) F_2\left(\kappa r_{ij}\right) \right\} \ , \tag{3}$$

with $F_1(y) = -y^2 K_2(2y)$ and $F_2(y) = 1/y^2 - y K_3(2y) - y^2 K_2(2y)$. Here α_{ij} is the angle between the vectors $\mathbf{e}_b$ and $\mathbf{r}_{ij} = \mathbf{r}_i - \mathbf{r}_j$, and K_n are modified Bessel functions. For $r \gg 1/\kappa$, the above expression is equivalent to the usual dipole-dipole interaction $\left[\propto \cos\left(2\alpha_{ij}\right)/r_{ij}^2\right]$.

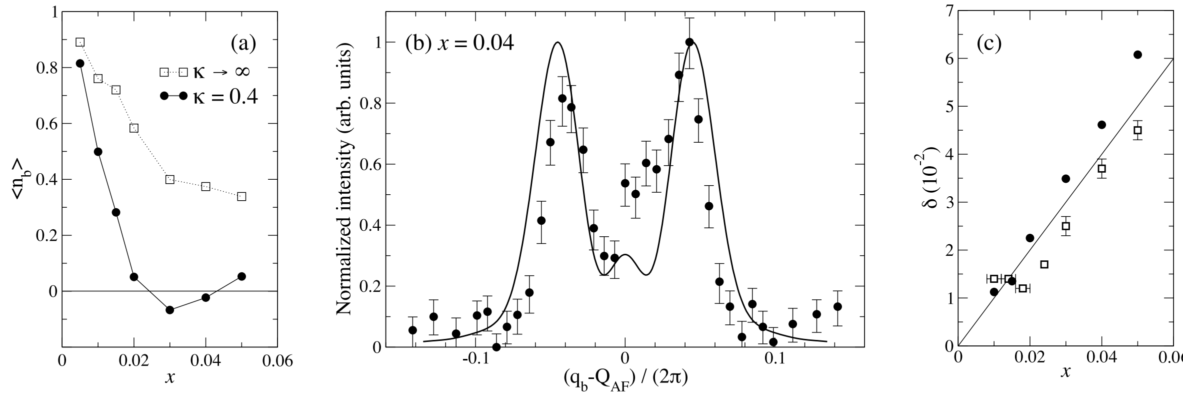

FIG. 3: *(a) $\langle n^b \rangle$ as a function of doping x. For $\kappa = 0.4$, Néel order is destroyed at $x_c \approx 0.02$, in agreement with experiments. For pointlike impurities ($\kappa \to \infty$), there is no phase transition at least up to $x = 0.05$. (b) Neutron scattering probability for $x = 0.04$. Full circles correspond to experimental observations. The curve represents our simulation, containing no fitting parameters. (c) Incommensurability δ (in reciprocal lattice units of the tetragonal lattice) as a function of doping. Our calculations (circles) are in good agreement with experimental measurements (squares).*

Spin-wave excitations in the spin-glass phase

It is necessary to derive the time-dependent Lagrangian. Naïvely

$$\mathcal{L}' = \frac{\chi_\perp}{2}\dot{\vec{n}}^2 + \sum_\alpha \left\{ \frac{i}{2}(\psi_\alpha^\dagger \dot{\psi}_\alpha - \dot{\psi}_\alpha^\dagger \psi_\alpha) \right\} - \mathcal{E} \ , \tag{4}$$

where $\chi_\perp \approx 0.5/(8J)$ is the perpendicular magnetic susceptibility and $\mathcal{E}$ is the static effective energy density. **However there is an additional non-trivial term!**

If we write in some coordinate frame $\vec{n} = (\sin\theta\cos\varphi, \sin\theta\sin\varphi, \cos\theta)$ where θ and φ smoothly depend on $\mathbf{r}$, then the Schrödinger equation for the two-component wave function $v_\alpha = (h_{\uparrow\alpha}, h_{\downarrow\alpha})^T$ reads

$$i\ \dot{v}_\alpha = -\sqrt{2}g(\vec{f}\cdot\vec{\sigma})v_\alpha \ ,$$

where $\vec{f} = (\theta', \varphi' \sin\theta, 0)$ and $F' = (\mathbf{e}_\alpha \cdot \nabla)F$. This is non-covariant form! To obtain the covariant form we use the identity

$$f^2 = (\theta')^2 + (\varphi')^2 \sin^2\theta = [\vec{n} \times (\mathbf{e}_\alpha \cdot \nabla)\vec{n}]^2 \ ,$$

Therefore, one can perform a unitary transformation U, $\psi_\alpha = U v_\alpha$, such that

$$U^\dagger (\vec{f} \cdot \vec{\sigma}) U = [\vec{n} \times (\mathbf{e}_\alpha \cdot \nabla)\vec{n}] \cdot \vec{\sigma} \ .$$

The Schrödinger equation for a single hole is thus transformed into

$$i\ \dot{\psi}_\alpha = -\sqrt{2} g\, [\vec{n} \times (\mathbf{e}_\alpha \cdot \nabla)\vec{n}] \cdot \vec{\sigma}\psi_\alpha - U^\dagger \dot{U} \psi_\alpha \ . \tag{5}$$

The corresponding Lagrangian has the form

$$\mathcal{L} \ = \ \frac{\chi_\perp}{2}\dot{\vec{n}}^2 + \sum_\alpha \left\{ \frac{i}{2}(\psi_\alpha^\dagger \dot{\psi}_\alpha - \dot{\psi}_\alpha^\dagger \psi_\alpha) - \frac{1}{2}\left(\psi_\alpha^\dagger \vec{\sigma} \psi_\alpha\right) \cdot [\vec{n} \times \dot{\vec{n}}] \right\} - \mathcal{E} \ . \tag{6}$$

It is important that this effective Lagrangian is also valid in the uniformly doped case. The additional $\vec{\sigma} \cdot [\vec{n} \times \dot{\vec{n}}]$ term is closely related to the Berry phase. It provides the fulfilment of Larmor's theorem: spins in a uniform magnetic field $\vec{B}$ precess with frequency $\vec{\omega} = \vec{B}$. We checked this statement using the effective Lagrangian in the presence of a uniform magnetic field,

$$\begin{aligned} \mathcal{L}_B = \frac{\chi_\perp}{2}\left(\dot{\vec{n}} - [\vec{n} \times \vec{B}]\right)^2 - \frac{\rho_s}{2}(\nabla \vec{n})^2 \\ + \frac{i}{2}(\psi^\dagger \dot{\psi} - \dot{\psi}^\dagger \psi) - \psi^\dagger \left[\frac{\beta \nabla^2}{2} + V(r)\right]\psi \\ - \frac{1}{2}\vec{\xi} \cdot [\vec{n} \times \dot{\vec{n}}] + \sqrt{2} g \vec{\xi} \cdot [\vec{n} \times \vec{n}'] + \frac{1}{2}(\vec{\xi} \cdot \vec{n})(\vec{B} \cdot \vec{n}) \ , \end{aligned}$$

where

$$\vec{\xi}(\mathbf{r}) = \psi^\dagger(\mathbf{r}) \vec{\sigma} \psi(\mathbf{r})$$

.

Uniform spiral approximation for the ground state

Mean-field approach:

$$\vec{\xi}_i = \Psi_i \vec{\sigma} \Psi_i = (0, 0, 1) \ ,$$

$$\vec{n} = (\cos \mathbf{Q} \cdot \mathbf{r}, \sin \mathbf{Q} \cdot \mathbf{r}, 0) \ .$$

After averaging over the impurity positions, we find the energy

$$\mathcal{E} = \rho_s/2Q^2 - \sqrt{2} g x (\mathbf{e}_b \cdot \mathbf{Q}).$$

The spiral pitch that minimizes this energy is given by

$$\mathbf{Q} = \frac{\sqrt{2} g x}{\rho_s} \mathbf{e}_b \ ,$$

and agrees well with accurate Monte Carlo simulations and experimental data. A uniform spiral is very similar to the true ground state and is thus a good starting point to describe excitations.

In-plane spin-wave excitations

An in-plane excitation is described by a small deviation $\varphi = \varphi(t, \mathbf{r})$ from the uniform spiral ground state:

$$\vec{n} = (\cos(\mathbf{Q} \cdot \mathbf{r} + \varphi), \sin(\mathbf{Q} \cdot \mathbf{r} + \varphi), 0) \ . \tag{7}$$

We assume that $q \lesssim \sqrt{x}$, where q is the typical momentum of the φ-field and $\sqrt{x}$ is the inverse average distance between impurities. In this limit, one can average over impurity positions and replace $\sum_i \rho(\mathbf{r} - \mathbf{R}_i) \to x$. After that the equation of motion for φ reads

$$\chi_\perp \ddot{\varphi} = \rho_s \nabla^2 \varphi \ .$$

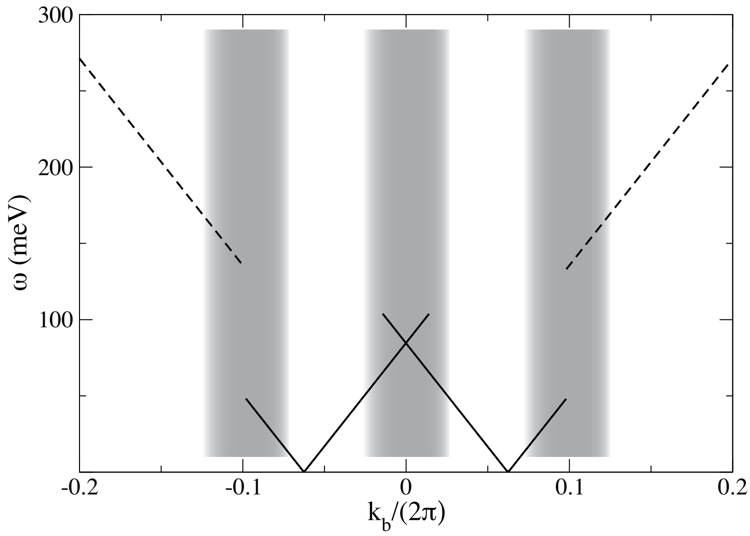

FIG. 4: Spectrum of in-plane spin waves excited in neutron scattering at doping $x = 0.05$. The momentum is directed along the orthorhombic b direction and $Q \approx 0.39$. There are two linear branches that start at $k_b = \pm Q$, that are broadened due to disorder and ultimately disappear at $|\mathbf{k} \pm \mathbf{Q}| \sim \sqrt{x}$. For larger momenta, spin waves reappear with usual dispersion of the Néel antiferromagnet. The frequency at the intersection $\mathbf{k}_b = 0$ scales linerly with doping.

The spectrum of in-plane excitations is thus exactly the same as the spin-wave spectrum in undoped LCO, $\omega = cq$, with the spin-wave velocity $c = \sqrt{\rho_s/\chi_\perp} \approx 1.66$. The corresponding Green's function of the φ-field is given by

$$G_{in} = \frac{\chi_\perp^{-1}}{\omega^2 - c^2q^2 + i0} \ .$$

The neutron scattering probability for unpolarized neutrons is given by

$$I_{in}(\omega, \mathbf{k}) \propto -\frac{1}{8\pi}\mathrm{Im}\left[G_{in}(\omega, \mathbf{k}-\mathbf{Q}) + G_{in}(\omega, \mathbf{k}+\mathbf{Q})\right]$$
$$= \frac{1}{16\chi_\perp\omega}\left[\delta(\omega - c|\mathbf{k}-\mathbf{Q}|) + \delta(\omega - c|\mathbf{k}+\mathbf{Q}|)\right] \ .$$

Out-of-plane spin-wave excitation

An out-of-plane excitation can be represented as a small deviation $n^z\,(\mathbf{r}, t)$ from the uniform spiral ground state

$$\vec{n} = (\sqrt{1-n_z^2}\cos\mathbf{Q}\cdot\mathbf{r}, \sqrt{1-n_z^2}\sin\mathbf{Q}\cdot\mathbf{r}, n_z)\ ,$$

Here $\Delta = 2\sqrt{2}gQ = 4g^2x/\rho_s$ is the energy required to flip a pseudospin .

The off-diagonal part of the Lagrangian gives rise to the pseudospin-flip vertices

$$\Gamma_{\uparrow\downarrow} = \frac{1}{\sqrt{\chi_\perp}}e^{i(\mathbf{Q}+\mathbf{q})\cdot\mathbf{R}_i}F(\mathbf{Q}+\mathbf{q})\left[\sqrt{2}g(Q-q_b)-\frac{\omega}{2}\right]\ ,$$
$$\Gamma_{\downarrow\uparrow} = \frac{1}{\sqrt{\chi_\perp}}e^{i(\mathbf{Q}-\mathbf{q})\cdot\mathbf{R}_i}F(\mathbf{Q}-\mathbf{q})\left[\sqrt{2}g(Q+q_b)+\frac{\omega}{2}\right]\ .$$

The Berry phase term is important for the out-of-plane spectrum because it leads to the additional terms $\pm\omega/2$ in this expression. The impurity form factor $F(\mathbf{p})$ is given by

$$F(\mathbf{p}) = \int d^2r\ \rho(\mathbf{r})e^{i\mathbf{p}\cdot\mathbf{r}} \approx 1 - \frac{3}{8}\frac{p^2}{\kappa^2}\ ,$$

The polarization operator is given by

$$P(\omega,\mathbf{q}) = x\left\{\frac{|\Gamma_{\uparrow\downarrow}|^2}{\omega-\Delta} + \frac{|\Gamma_{\downarrow\uparrow}|^2}{-\omega-\Delta}\right\}$$
$$\approx -c^2\left\{Q^2 + \frac{q_b^2}{1-\omega^2/\Delta^2} - \frac{3}{4\kappa^2}\left[(Q^2-q_b^2)^2 + q_a^2(Q^2+q_b^2)\right]\right\}\ .$$

Including single-loop corrections, the Green's function of the n_z-field reads

$$G_{out} = \frac{\chi_\perp^{-1}}{\omega^2-\omega_{\mathbf{q}}^2-P(\omega,\mathbf{q})}\ ,\quad \omega_{\mathbf{q}}^2 = c^2(q^2+Q^2)\,.$$

The excitation spectrum is given by poles of the Green's function. We find two branches

$$\Omega_{1,\mathbf{q}} \approx c\sqrt{\frac{q_a^2 + \frac{3}{4\kappa^2}\left[(Q^2 - q_b^2)^2 + q_a^2(Q^2 + q_b^2)\right]}{1 + \frac{c^2 q_b^2}{\Delta^2}}} \ ,$$
$$\Omega_{2,\mathbf{q}} \approx \Delta + \frac{c^2 q_b^2}{2\Delta} \ .$$

The lower branch vanishes at $\mathbf{q} = \pm\mathbf{Q}$, in accordance with the Goldstone theorem, while the upper branch has a gap Δ.

The neutron scattering probability defined by the interaction (**??**) reads

$$I_{out}(\omega, \mathbf{q}) \propto -\frac{1}{4\pi}\mathrm{Im}\ G_{out}(\omega, \mathbf{q}) \tag{8}$$
$$\approx \frac{1}{8\chi_\perp \omega}\left[Z_\mathbf{q}\delta(\omega - \Omega_{1,\mathbf{q}}) + (1 - Z_\mathbf{q})\delta(\omega - \Omega_{2,\mathbf{q}})\right] \ ,$$

with the quasi-particle residue

$$Z_\mathbf{q} = \frac{1}{1 + \frac{c^2}{8g^2}\frac{q_b^2}{Q^2}} \ .$$

The upper branch has a practically vanishing spectral weight at small q. Interestingly, the ratio between the predicted intensities for the low-frequency in- and out-of-plane spin waves is $I_{out} : I_{in} = 2$. Such a difference should be detectable in experiments.

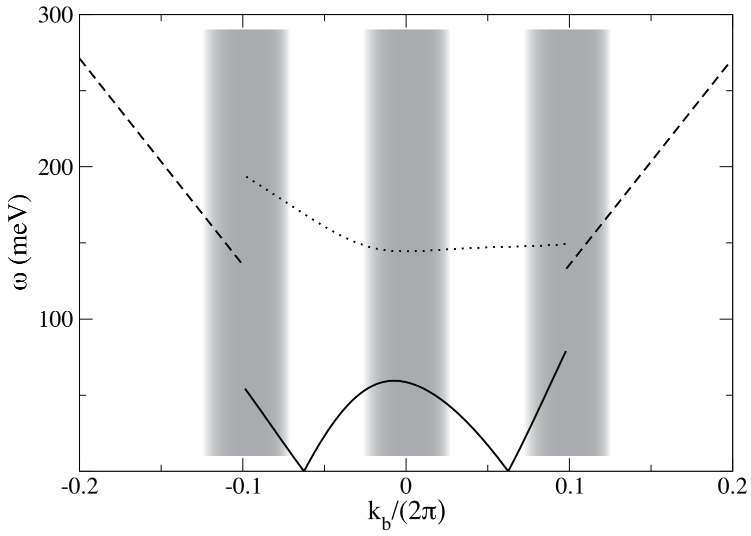

FIG. 5: Spectrum of out-of-plane spin-wave excitations at doping $x = 0.05$. The Momentum is directed along the orthorhombic b direction. The inverse radius of the impurity wave-function is $\kappa = 0.4$ and $Q \approx 0.39$. The upper branch has a very small spectral weight and it thus difficult to observe in neutron scattering. At larger momenta, the spin waves reappear with usual dispersion of the Néel antiferromagnet. The frequency at the top of the dome at $\mathbf{k}_b = 0$ scales quadratically with doping.

Conclusion

We have derived the low-energy effective field theory of the t-J model in the limit of small doping.

We have calculated the spin-wave excitations in the disordered spin spiral state of $La_{2-x}Sr_xCuO_4$ (the spin-glass phase), which has a coplanar spin structure.

For the in-plane spectrum, we have found the usual linear spin-wave dispersion, while the out-of-plane modes have been shown to exhibit non-trivial doping dependent features.